JOURNAL OF MATERIALS SCIENCE 35 (2000) 4193–4199

Microstructure and secular instability of the $(Ti_{1-x},Al_x)N$ films prepared by ion-beam-assisted-deposition

T. SUZUKI*,‡, Y. MAKINO
Joining and Welding Research Institute, Osaka University, 11-1, Mihogaoka, Ibaraki, Osaka 567-0047, Japan
E-mail: suzuki@vos.nagaokaut.ac.jp

M. SAMANDI
Surface Engineering Research Center, University of Wollongong, Northfields Avenue Wollongong 2500, Australia

S. MIYAKE
Joining and Welding Research Institute, Osaka University, 11-1, Mihogaoka, Ibaraki, Osaka 567-0047, Japan

$(Ti_{1-x},Al_x)N$ films were prepared by ion beam assisted deposition (IBAD). The films were synthesized by depositing titanium and aluminum metal individual vapor under simultaneous bombardment with nitrogen ions in the energy range of 0.2–20 keV with the (Ti_{1-x},Al_x)/N transport ratio in the range of 0.5–2.0. The films were formed onto Si(111) wafers at room temperature. Structural characterization of the films was performed with x-ray diffraction and selected area electron diffraction. The crystalline structure of the $(Ti_{0.64},Al_{0.36})N$ and $(Ti_{0.33},Al_{0.67})N$ films were found to be a metastable single-phase B1-NaCl structure. The $(Ti_{0.29},Al_{0.71})N$ films revealed a two-phase mixture consisting of NaCl and würtzite structural phases. The AlN solubility limit into TiN, which approximately equal with x value, calculated by using electron theory was about $x = 0.65$, which shows good agreement to the experimental results. Phase separation after half a year of aging at room temperature in air was observed on the $(Ti_{0.33},Al_{0.67})$ films whose AlN content is close to the solubility limits.

1. Introduction

Recently, the synthesis of $(Ti_{1-x},Al_x)N$ films have been attracting an increasing interest as a mean of obtaining wear-protective coatings with higher oxidation resistance at elevated temperatures [1, 2] and an improved performance in machining operations [3]. $(Ti_{1-x},Al_x)N$ coatings with such desirable properties may provide a promising alternative to conventionally used TiN coatings [4]. These $(Ti_{1-x},Al_x)N$ film have been prepared by using a variety of physical vapor deposition (PVD) techniques [1–7].

In the equilibrium Ti-Al-N ternary-phase diagram, Ti, Al and N appear to have essentially no solubility in AlN, TiN and TiAl, respectively, and Ti_2AlN, Ti_3AlN and $Ti_3Al_2N_2$ are found as the only equilibrium ternary phases [8]. So far the investigations on the variation of the microstructure and the metastable phases in the $(Ti_{1-x},Al_x)N$ films by PVD techniques have been mainly discussed as a function of the aluminum content in the films.

This study aims to investigate the microstructure of the $(Ti_{1-x},Al_x)N$ films prepared using IBAD technique, which exhibits advantages in the controllability of the energy, and, the ion to atom ratios, over a variety of PVD. The $(Ti_{1-x},Al_x)N$ films are prepared by vapor deposition of Ti and Al individually under simultaneous bombardment with N ions in the energy range of 2–20 keV. Crystalline structure of the films was characterized using x-ray diffraction (XRD) and selected area diffraction (SAD). Secular instability was also studied.

2. Experimental

A compact IBAD system with a bucket-type 2.45 GHz electron-cyclotron-resonance ion source and an electron beam evaporation source was used for the preparation of the $(Ti_{1-x},Al_x)N$ films. Details of the deposition system have been described elsewhere [9]. Acceleration voltage of the extracted nitrogen ions was varied in the range of 0.2–20 kV. The ion current measured using a Faraday cup with an entrance aperture

* Author to whom all correspondence should be addressed.
‡ *Present Address*: Extreme Energy Density Research Institute, Nagaoka University of Technology, 1603-1 Kamitomioka, Nagaoka, Niigata 940-2188, Japan.

of 3 cm diameter was typically 0.7 mA; i.e., the ion current density onto a substrate was 0.1 mA/cm^2. The base pressure of the deposition system, evacuated with a 1500 l/s cryopump, was 9×10^{-5} Pa. The working pressure of nitrogen during the ion source operation was $2–3 \times 10^{-3}$ Pa. The substrate temperature was limited to be less than 250 °C by a water cooling system.

The $(Ti_{1-x},Al_x)N$ films were prepared on Si (111) wafers by depositing the evaporated titanium and aluminum individually under simultaneous bombardment with N ions. The elemental composition of the deposited films was measured using energy-dispersive X-ray spectroscopy (EDX) and X-ray fluorescence (XRF) analysis. The atomic percent of aluminum in the films was measured to be higher than that in the evaporation source, possibly because of the lower melting point for aluminum than titanium. The transport ratio $(Ti_{1-x},Al_x)/N$ was varied in the range of 0.5–2.0.

The crystalline structure of the films were characterized by using XRD and SAD. XRD measurements were performed by using a diffractometer (Rigaku Corp. RINT2000 series) with Cu K_α radiation. Glancing-incidence thin-film optics were employed with the theta drive locked at 1.00°.

TEM observations were also performed to analyze the phases that consisted. For these investigations, the films with a thickness of ~600 Å were deposited onto electron-transparent Si (111) substrates. The preparation of these specific substrates was accomplished before the film deposition, which consisted of grinding, followed by etching in hydrofluoric acid to obtain electron-transparent specimens. This method for preparing TEM samples has advantages that which require thinning processes after the deposition of the films. The method enables the plan-view observations in a very thin layer (possibly ~500 Å) of as-deposited films without degrading and/or changing the microstructure due to chemical-etching and/or ion-milling processes. The post-thinning process with ion milling technique may simply add significant ambiguities to the examinations of the microstructure that resulted from the ion-beam irradiation during film growth. TEM observations and SAD measurements were performed by using HITACHI H800 and JEOL 2010 electron microscope operated at 200 kV.

Microhardness measurement was carried out by a UMIS2000 using a Berkovich (Triangular pyramid) indenter [10, 11]. The indentation load was incrementally increased in 30 steps and at each step the indentation depth was measured. Even at the lowest load (1 mN) the indenter penetrated about 500–600 Å. Since the coating thickness is about 1000 Å indentations at higher loads were significantly influenced by the substrate and are not used for further analysis in this work.

3. Results and discussion

3.1. AlN content dependence on the structures

The phase of the $(Ti_{1-x},Al_x)N$ films for various x value was identified by using SAD. Typical SAD patterns from the $(Ti_{1-x},Al_x)N$ films for $x = 0.36, 0.67, 0.71$ and 0.84 are shown in Fig. 1a–d, respectively. Here the films were prepared with 2 keV N ion beam at a transport ratio $(Ti_{1-x},Al_x)/N$ of 2.0, and the composition of Al to metal (Ti + Al) in the films was obtained from EDX measurements.

The SAD patterns from the films for $x = 0.36$ and 0.67 show a single-phase B1-NaCl structure which is typical for TiN. It should be noted that Ti-Al intermetallic compounds such as Ti_3Al and TiAl and $TiAl_3$, or solid solutions such as α-Ti, β-Ti dissolving Al are not observed, which is in contrast to our previous IBAD study [12] to prepare the Ti-Al films with (Ti + Al) vapor deposition under simultaneous Ar-ion-beam bombardment. Possibly, this is attributed to the reactivity of N ions, which may tend to stabilize the Ti-Al-N system as a metastable nitride rather than in a multiphase mixture composed of the intermetallic phases together with nitride phases. Then a question arises whether Al is actually incorporated or not in the single-phase NaCl structure typical of TiN. To answer this question, elemental mappings constructed from Ti and Al signals in EDX are compared to the plan-view TEM images from the films. As a result the spatial distributions of Ti and Al atoms are found to be homogeneous over the entire film region and obviously consistent with the plan-view TEM images.

With increasing x value, the film for $x = 0.71$ shows a two-phase mixture consisting of NaCl and würtzite crystalline phases, as being found in Fig. 1c. The variation of the phases from the B1 structure to the two-phase mixture (NaCl and wurtzite structures) with increasing x value in the Ti-Al-N system is consistent with the result obtained from the films deposited using the cathodic arc ion plating [6] and the dual-target magnetron sputtering [7]. The SAD pattern from the film for $x = 0.84$ shows a single würtzite.

The phase diagram of $(Ti_{1-x},Al_x)N$ films for various x value prepared by IBAD with 2 keV N ion beam at a transport ratio $(Ti_{1-x},Al_x)/N$ of 2.0 is summarized in Fig. 2. The structures of the films for $x = 0–0.67$ are single B1-NaCl structures. When x value exceeds 0.71, two phases structures (NaCl + würzite) were observed. A further increase in x value above ~0.84 resulted in shingle-phase B4-würtzite structure.

We have reported a dependence of AlN content on the lattice parameter of the $(Ti_{1-x},Al_x)N$ films in our previous IBAD study [13]. The lattice parameters of the B1-single phase $(Ti_{1-x},Al_x)N$ films were decreased with increasing AlN content, probably caused by Al substituting to Ti in the TiN lattice.

3.2. Comparison of the AlN solubility limit with the theoretical prediction

In this subsection, the experimental solubility limit of AlN was compared with the predicted one, which is calculated by using crystal structure map based on the two band parameters.

The prediction of AlN solubility limit for B1 TiN is quite important for the practical applications, because the B1 single phase $(Ti_{1-x},Al_x)N$ films with the high AlN content are considered to obtain excellent oxidation resistance and hardness which are necessitated for

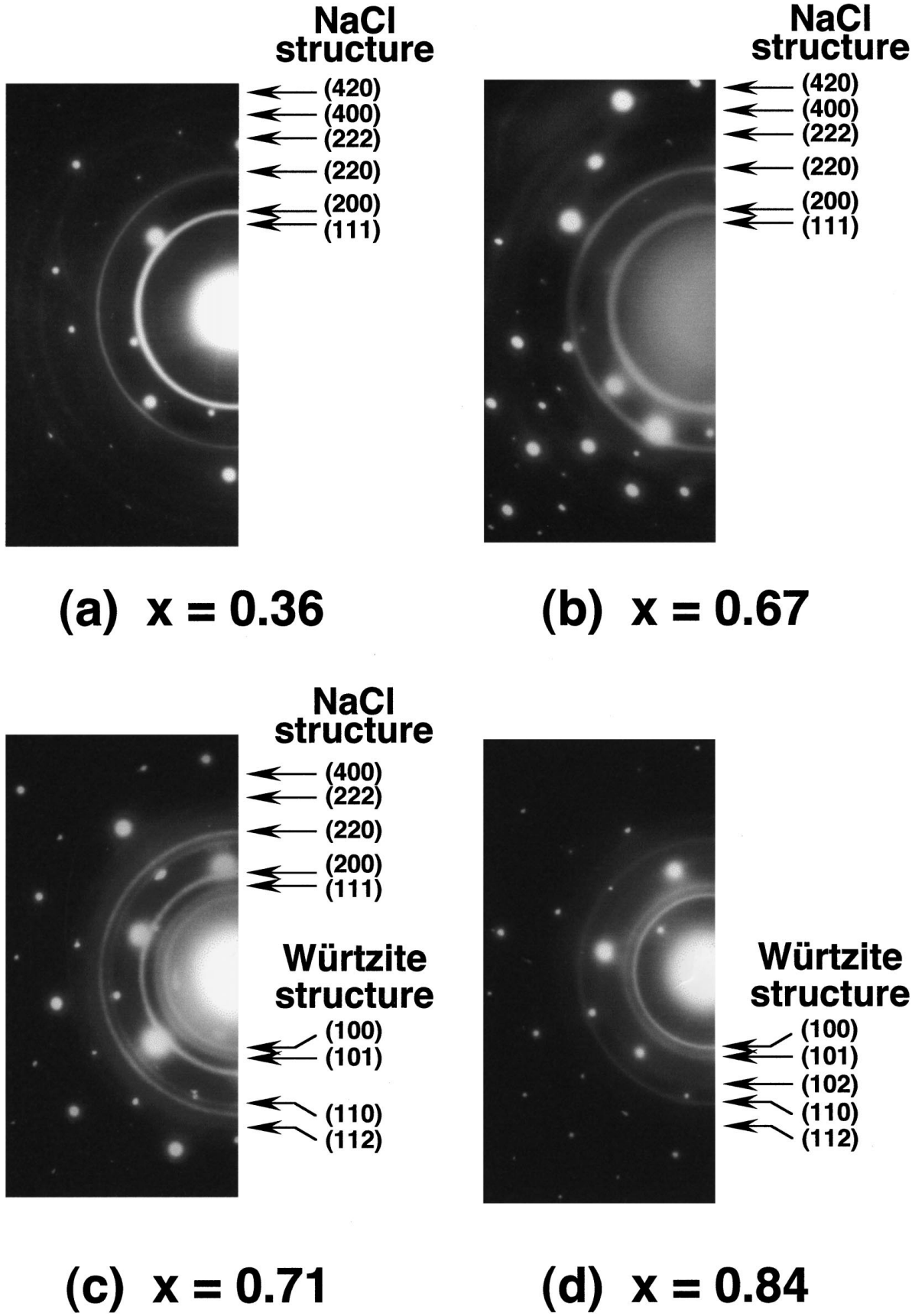

Figure 1 Typical SAD rings of the $(Ti_{1-x},Al_x)N$ films with $x =$ (a) 0.36, (b) 0.67, (c) 0.71 and (d) 0.84. The films were prepared with 2 keV N ion beam at the transport ratio $(Ti_{1-x},Al_x)/N = 2.0$. The net patterns were corresponded to the Si substrate.

the application of wear coating. Although we studied this solubility limit experimentally as shown in Fig. 2, we compared it with the theoretical model based on the crystal structure mapping constructed from two band parameters.

In the previous paper [14], it has been indicated that the critical solubility of AlN into transition metal nitrides with B1 crystal structure can be predicted by the two band parameters and the structural map based on these parameters. The critical solubility corresponds

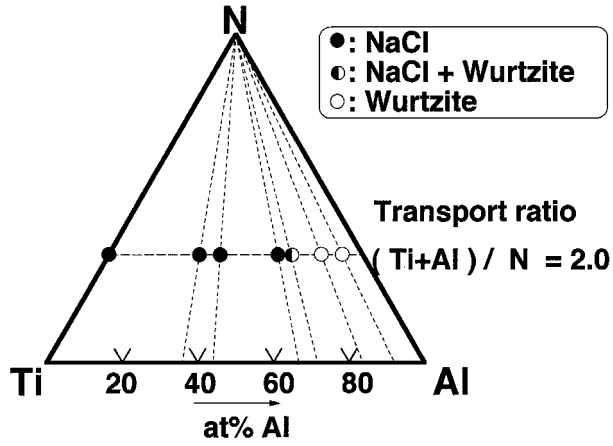

Figure 2 Phase diagram of the $(Ti_{1-x},Al_x)N$ films prepared by IBAD at the transport ratio $(Ti_{1-x},Al_x)/N$ of 2.0.

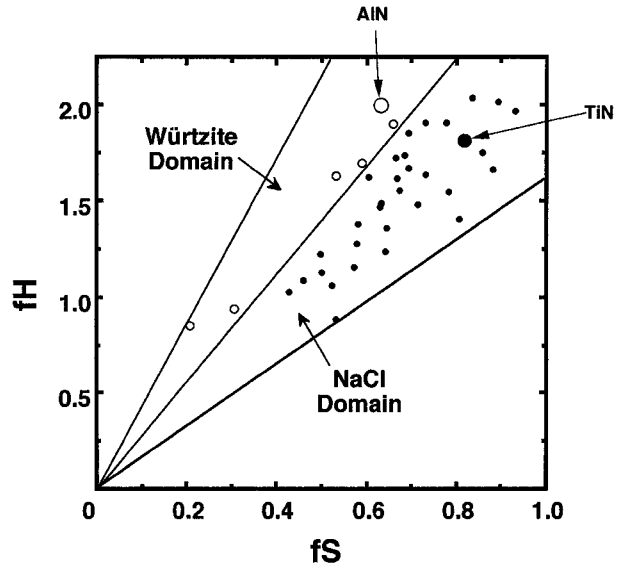

Figure 3 Structural map for AB compounds with B1 and B4 structures by two band parameters.

to the critical composition at which the pseudobinary nitrides containing AlN transform the B1 structure to a B4 one. Here, the prediction method to calculate the critical composition for the phase transition in the pseudobinary nitride is briefly explained because it is necessary to compare the predicted composition with the experimental result on the Ti-Al-N films.

Using the two band parameters based on the pseudopotential radii of Zunger [15] and the bond orbital model [16], the structural map for the several fundamental crystal structures such as B1(NaCl), B2(CsCl), B3(zincblende) and B4(würtzite) type can be constructed in a two dimensional expression. The structural coordinates are constructed by the two band parameters {hybrid function (H) and gap reduction parameter (S)} and compositional factor (f_{inv}), and those for sp bonding are expressed as follows;

$$H(\text{sp}) = \left(\frac{\alpha_s}{n_{av}}\right)^{1/2} + \left(\frac{\alpha_p}{n_{av}}\right)^{1/2},$$

$$S(\text{sp}) = \left[\frac{\{S_{sp}(A) + S_{sp}(B)\}}{n_{av}}\right]^{1/2}$$

$$f_{inv} = \frac{(4N_A N_B x_A x_B)}{(N_A x_B + N_A x_B)^2}$$

where $\alpha_s = |(Z/r_s)_A^{1/2} + (Z/r_s)_B^{1/2}|$, $\alpha_p = |(Z/r_p)_A^{1/2} + (Z/r_p)_B^{1/2}|$, $S_{sp} = |(Z/r_s)_i^{1/2} + (Z/r_p)_i^{1/2}|$, ($i$, A or B), and r_s, r_p, n_{av} and Z are the Zunger's pseudopotential radii of s and p electrons, the average quantum number and valence, respectively. Further, N_A and N_B are the valence electron numbers of A and B atoms, and x_A and x_B are the atomic fractions of A and B atoms, respectively. When B atom is a transition metal, α_d and S_{sd}(B) are used instead of α_p and S_{sp}(B) in the above described equations, where $\alpha_d = |(Z/r_s)_A^{1/2} + (Z/r_d)_B^{1/2}|$ and $S_{sd} = |(Z/r_s)_B^{1/2} + (Z/r_p)_B^{1/2}|$. The two band parameters and compositional factor were explained in details elsewhere [17, 18]. In general, S corresponds to a band gap reduction due to the formation of crystalline state, while H corresponds to the contributions of s and p electrons to the difference between bonding and anti-bonding levels.

The critical composition for the phase transition of $(Ti_{1-x},Al_x)N$ films from the B1 type crystal structure to the B4 one was determined by the boundary line between B1 and B4 structures and the positions of TiN and AlN in the structural map as shown in Fig. 3. The numerical value (x) is calculated by the following equation;

$$x = \frac{\{f_{\text{inv(MN)}}(2.78 S_{MN} H_{MN})\}}{\{f_{\text{inv(AlN)}}(H_{AlN} - 2.78 S_{AlN}) - f_{\text{inv(MN)}}(H_{MN} - 2.78 S_{MN})\}}$$

where H_{MN}, S_{MN} and $f_{\text{inv(MN)}}$ are the hybrid function, gap reduction parameter and compositional factor of transition metal nitride (MN), and H_{AlN}, S_{AlN} and $f_{\text{inv(AlN)}}$ are those of AlN, respectively. The numerical value of 2.78 is the slope of the boundary line between B1 and B4 domains in the structural map.

The values of critical solubility of AlN into titanium nitrides with B1 structure are 65 atomic percent. These results mean that the phase is B1 structure typical for TiN below 65 at.% AlN, and is B4 structure typical for AlN above 65 at.% AlN. Taking into account the accuracy of EDX composition measurement, this prediction of AlN solubility limit into TiN (65 at.%) shows a good agreement with the experimental results (67 at.%) from the viewpoint of the AlN solving limitation.

This prediction indicated that the phase transforms B1-single to B4-single directly with increasing AlN at the 65 at.%. But many researchers reported that there is the composition range of B1 + B4 mixed structure [6, 7], also shown in Fig. 2 in our results. We consider that this discrepancy was caused by the fact that this prediction could not include the factor concerning the degree of non-equilibrium such as a temperature, cooling

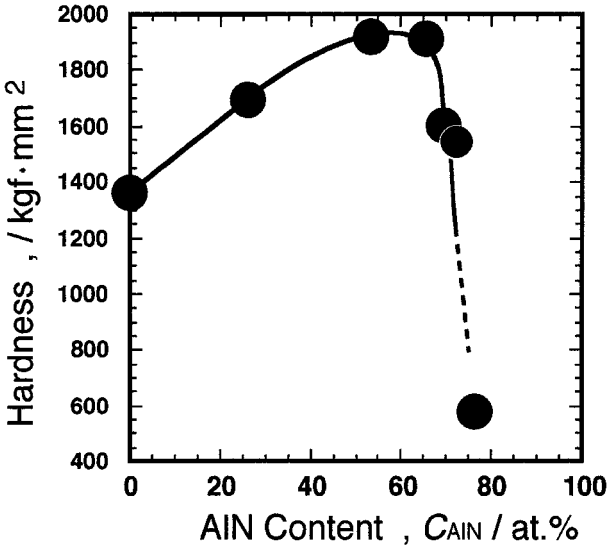

Figure 4 The dependence of hardness of the $(Ti_{1-x},Al_x)N$ films on AlN content.

rate, and the pressure effects of ions or other considerations. Also the nonstoichiometry (Metal to Nitrogen) is considered to be another reason why this discrepancy arise. We additionally remark that it is possible to obtain the single B1 structured $(Ti_{1-x},Al_x)N$ film with the critical composition (65 at.% AlN) by ideal processes which are able to achieve the ultimate condition.

We discussed the details of this theory in the reference [17–19] including its application to other pseudobinary nitrides system such as $(Cr_{1-x},Al_x)N$ [20, 21] or intermetallic compounds [22].

3.3. Microhardness

The microhardness of the $(Ti_{1-x},Al_x)N$ films for various x value are shown in Fig. 4. The hardness increased with x up to about 0.65, and decreased rapidly within the composition range of the (NaCl + würtzite) mixed structure.

Although increasing hardness caused by substitution of Al atom to Ti atom in B1 type TiN lattice has been reported by some researchers [6, 23, 24], the explanation on the hardening mechanism has not been discussed in details. We suggest that one solution is to use the solution hardening mechanism. Here, we consider the hardening mechanism from the stand point of mechanical property.

Cohen reported the relation between bulk modulus (GPa) and the nearest neighbor distance (Å) of AB compounds with tetrahedral coordination [25]. This relation is expressed as follows;

$$B = 1761d^{-3.5}$$

With decreasing the interatomic distance, the potential for affecting the atoms increased; in other words, the bonding strength between A-B is increased. Although there is some problem for applying this relation to the Ti-Al-N system directly because of neglecting the effects of d electrons, bulk moduli increases with decreasing interatomic distance [26]. Decreasing of interatomic distance caused by the aluminum substituting to Ti into the TiN lattice were reported by many researchers, and we also obtained the same results as shown in the reference [13]. Thus the hardening of Ti-Al-N pseudobinary films can be interpreted by the increase of their bulk moduli.

3.4. Secular structure instability (room temperature-aging behavior)

The boundary of x value between B1 single phase and B1 + B4 mixture phase was found to be about 0.65 as shown in the experimental results (Fig. 2) and the prediction by using structure mapping obtained from the band parameters. Although the TEM observation of $(Ti_{0.33},Al_{0.67})N$ showed B1-NaCl single crystal structure even after passing one month (Fig. 1b), the structure changed into the NaCl + würtzite mixed phase after half a year has passed at room temperature in air. Fig. 5a and b shows the comparison of the SAD patterns taken from the same sample before and after half a year room temperature aging (RT-aging), respectively. It should be noted that these SAD patterns were typical ones at each of the TEM observation. The SAD pattern taken before RT-aging as seen in Fig. 5a shows that the diffraction rings from the film were broadening. This broadening of the diffraction rings was considered to be caused by, 1) the strain in the films, 2) the certain width of the lattice parameters caused by the composition fluctuation of the matrix.

It is considered that the films have not so large stress as cubic boron nitride films do, because no film bending was observed as prepared onto the Si substrates. The $(Ti_{1-x},Al_x)N$ films with the composition close to aluminum solubility limit are supposed to be very unstable, so that the spinodal decomposition may arise in order to decrease the free energy of the matrix.

There may be high possibility of spinodal decomposition. A schematic path for spinodal decomposition is shown in Fig. 6 as example of case at the $(Ti_{0.33},Al_{0.67})N$ films close to the critical composition.

Should spinodal decomposition in the $(Ti_{1-x},Al_x)N$ films arise, an aluminum composition perturbation results; i.e. Al-rich and -poor areas are made. Al-poor areas still would exist as a B1-$(Ti_{0.33-\delta},Al_{0.67+\delta})N$, otherwise a Al-rich area would precipitate as a B4-$(Ti_{0.33+\delta},Al_{0.67-\delta})N$. The latter is AlN where Ti substituting in Al into AlN lattice. As a result, taking such a decomposition path, the SAD patterns of the two phases were observed as shown in Fig. 5b. Finally, these two phases would change into equilibrium TiN and AlN, respectively.

Furthermore, oxidation was considered to be the mechanism which promoted the spinodal decomposition. The sample prepared onto the Si substrates and RT-aged for about 2 years shows the broadening diffraction peak at the XRD pattern as shown by the arrow in Fig. 7. Also in the TEM observations, broadening patterns were observed as shown in Fig. 8. These broadening patterns were possibly due to the existence of titanium oxide. The $(Ti_{1-x},Al_x)N$ films prepared by IBAD include about 10 atomic percent oxygen which was contaminated during the deposition. This oxygen

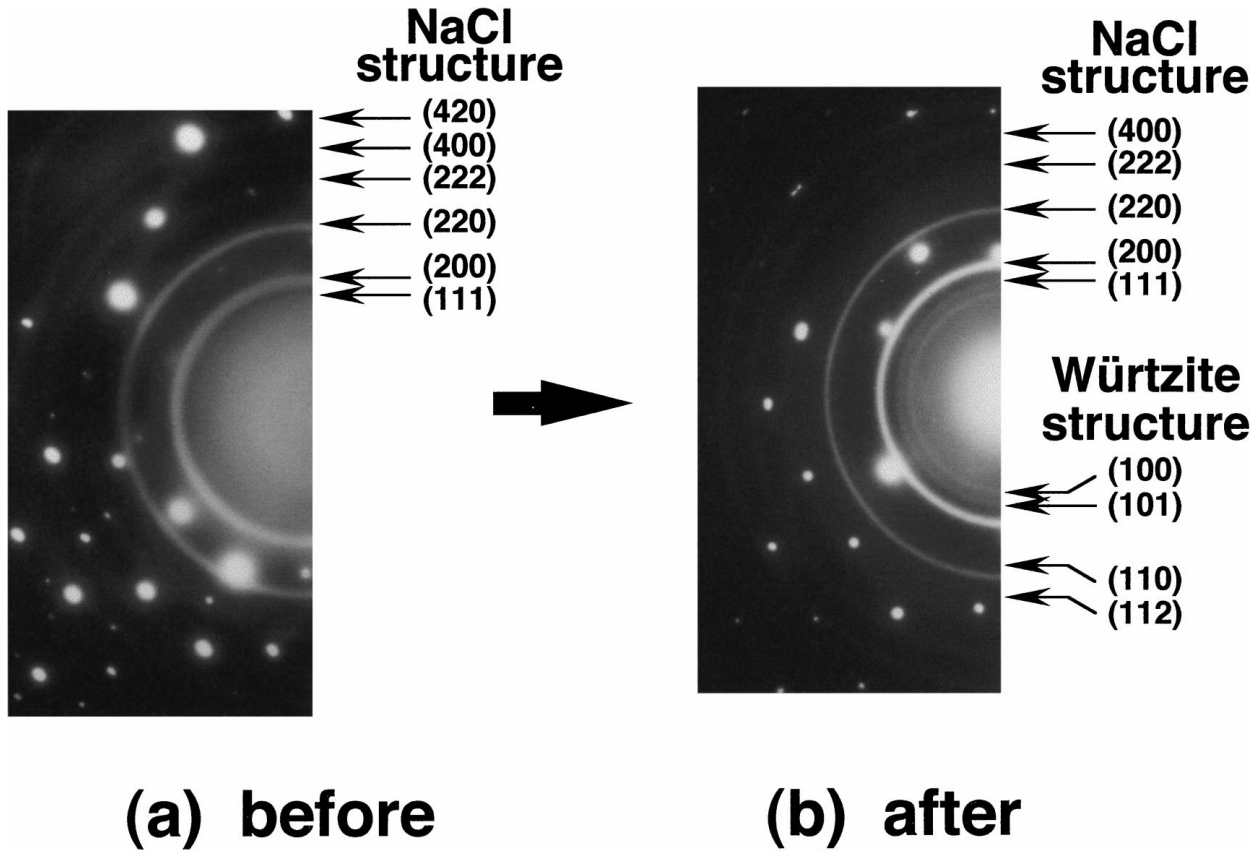

Figure 5 The comparison of typical SAD patterns from the $(Ti_{0.33},Al_{0.67})N$ sample at the observations of (a) before, and (b) after half a year RT-aging.

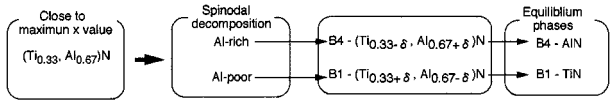

Figure 6 A schematic path for spinodal decomposition of the $(Ti_{0.33},Al_{0.67})N$ films.

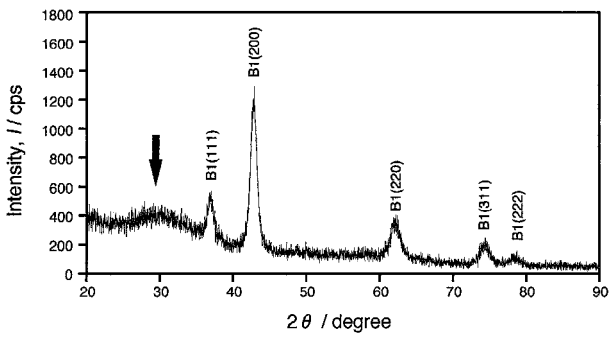

Figure 7 XRD patterns from the $(Ti_{1-x},Al_x)N$ sample which was RT aged for about 2 years.

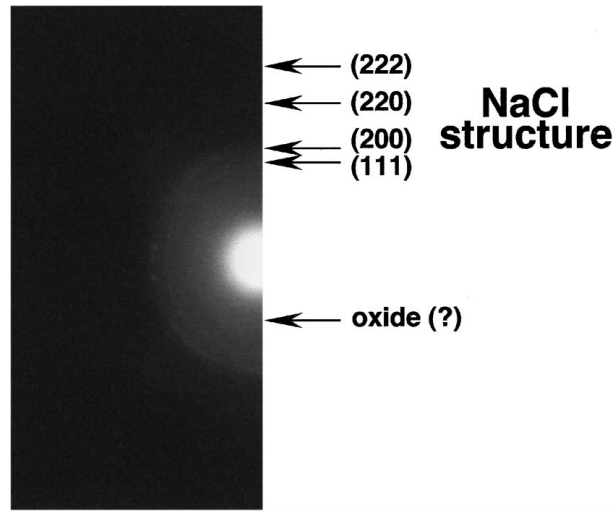

Figure 8 SAD patterns from the $(Ti_{1-x},Al_x)N$ sample which was RT aged for about 2 years.

that existed in the films causes the oxide formation, also oxidation during RT-aging occurred considerably easily, because of the diffusion of oxygen seems easy to obtain due to the small crystalline as can be seen from the fact that SAD did not show *spotty patterns* but show *rings patterns*.

Ichimura *et al*. reported that TiO_2 was formed at the first stage of the oxidation process of the $(Ti_{1-x},Al_x)N$ films [5]. Once the $(Ti_{1-x},Al_x)N$ films oxidized, x value of $(Ti_{1-x},Al_x)N$ films would increase relatively. In the case of the $(Ti_{1-x},Al_x)N$ with the critical composition ($x = \sim 0.65$), the aluminum composition would easily exceed the solubility limit. As a result, the NaCl-single phase separated into two phases (NaCl + würtzite).

$(Ti_{1-x},Al_x)N$ films are synthesized with various methods by many researchers. The $(Ti_{1-x},Al_x)N$ films for critical x value are expected to obtain the best oxidation resistance and the hardness. In a practical usage of the $(Ti_{1-x},Al_x)N$ films, the films will suffer thermal hysteresis for a long-time service. We worried about the $(Ti_{1-x},Al_x)N$ films with high x value would change their consisted phase after a long period usage, and the elevated temperatures promoted a spinodal

decomposition and impaired the oxidation resistance and the hardness. It should be noted that research about secular instability and characteristic degradation is required.

4. Summary

The $(Ti_{1-x},Al_x)N$ films were prepared by ion-beam-assisted-deposition. The $(Ti_{1-x},Al_x)N$ films for $x = 0.36$ and 0.67 atomic percent revealed a metastable single-phase B1-NaCl structure. With increasing aluminum content, the $(Ti_{0.29}, Al_{0.71})N$ films were found to be a two-phase mixture consisting of NaCl and würtzite structure phases, while the $(Ti_{0.16}, Al_{0.84})N$ showed single-würtzite structure.

The AlN solubility limit into TiN was studied experimentally and theoretically. Both values of AlN solubility limit shows close agreement; i.e. 67 at.% AlN by the experimental results, 65 at.% AlN by the theoretical calculation.

The hardness of the $(Ti_{1-x},Al_x)N$ films increased with x up to about 0.60, and decreased rapidly caused by the existence of B4 structure as a second phase. The hardening mechanism resulting in the Al solving into TiN lattice was discussed by the decrease of lattice parameters using Cohen's theory.

In the Ti-Al-N system, there may be the question of spinodal decomposition which reduced the intrinsic properties for the application of wear protective coatings such as hardness and oxidation resistance.

Acknowledgements

The authors wish to express our thanks to T. Kubo, K. Okuda (Rigaku Corp.) for the measurement of XRF and the analysis of XRD, and A. Nishimoto, M. Takahashi and M. Maeda (JWRI, Osaka Univ.), T. Sakata and H. Mori (Res. Center for UHVEM, Osaka Univ.) for the TEM observations, and Xinyang Li (Univ. of Wollongong) for the microhardness measurement.

References

1. M. WITTMER, J. NOSTER and H. MELCHIOR, *J. Appl. Phys.* **52** (1981) 6659.
2. O. KNOTEK, M. BÖHMER and T. LEYENDECKER, *J. Vac. Sci. Technol.* **A4** (1986) 2695.
3. T. LEYENDECKER, O. LEMMER, S. ESSER and J. EBBERINK, *Surf. Coat. Technol.* **48** (1991) 175.
4. W. D. MÜNZ, *J. Vac. Sci. Technol.* **A4** (1986) 2717.
5. H. ICHIMURA and A. KAWANA, *J. Mater. Res.* **8** (1993) 1093.
6. T. IKEDA and H. SATOH, *Thin Solid Films* **195** (1991) 99.
7. U. WAHLSTRÖM, L. HULTMAN, J.-E. SUNDGREN, F. ADIBI, I. PETROV and J. E. GREENE, *ibid.* **235** (1993) 62.
8. J. C. SCHUSTER and J. BAUER, *J. Solid State Chem.* **53** (1984) 260.
9. S. MIYAKE, K. HONDA, T. KOHNO, Y. SETSUHARA, A. CHAYAHARA and M. SATOU, *J. Vac. Sci. Technol.* **A10** (1992) 3253.
10. T. J. BELL, J. S. FIELD and M. V. SWAN, *Materials Forum* **17** (1993) 127.
11. T. J. BELL, A. BENDELI, J. S. FIELD, M. V. SWAN and E. G. THWAITE, *Metrologia* **28** (1991/92) 463.
12. Y. SETSUHARA, H. OHSAKO, Y. MAKINO and S. MIYAKE, *Surf. Coat. Technol.* **66** (1994) 495.
13. Y. SETSUHARA, T. SUZUKI, Y. MAKINO, S. MIYAKE, T. SAKATA and H. MORI, *ibid.* **97** (1997) 254.
14. Y. MAKINO, Y. SETSUHARA and S. MIYAKE, in Proc. 9th Intl. Conf. on Ion Beam Modification of Materials, Canberra, Australia, February, 1995, p. 735.
15. A. ZUNGER, *Phys. Rev.* **B22** (1980) 5839.
16. W. A. HARRISON, "Electronic Structure and The Properties of Solids" (Freeman, San Francisco, CA, 1980) Ch. 3.
17. Y. MAKINO, *Mater. Sci. and Eng.* **A192/193** (1995) 77.
18. *Idem., Intermetallics* **2** (1994) 55.
19. *Idem., Mater. Sci. and Eng.* **A179/180** (1994) 238.
20. A. SUGISHIMA, H. KAJIOKA and Y. MAKINO, *Surf. Coat. Technol.* **97** (1997) 590.
21. Y. MAKINO and K. NOGI, *ibid.* **98** (1998) 1008.
22. Y. MAKINO, *Mater. Sci. Eng.* **A192/193** (1995) 77.
23. J. R. ROOS, J. P. CELIS, E. VANCOILLE, H. VELTROP, S. BOELENS, F. JUNGBLUT, J. EBBERINK and H. HOMBERG, *Thin Solids Films* **193/194** (1990) 547.
24. Y. TANAKA, T. M. GÜR, M. KELLY, S. B. HAGSTROM and T. IKEDA, *ibid.* **228** (1993) 238.
25. M. L. COHEN, *Phys. Rev.* **B32** (1985) 7988.
26. Y. MAKINO, *J. Alloys and Comp.* **242** (1996) 122.

Received 17 June 1998
and accepted 16 February 2000